Applied Physics A (2020) 126:492
https://doi.org/10.1007/s00339-020-03639-7

Applied Physics A
Materials Science & Processing

Growth of [010] oriented urea-doped triglycine sulphate (Ur-TGS) single crystals below and above Curie temperature (T_c) and comparative investigations of their physical properties

Muthu Senthil Pandian[1] · Sunil Verma[2,3] · P. Ramasamy[1] · G. Singh[2,3] · S. M. Gupta[2,3] · V. S. Tiwari[2,3] · A. K. Karnal[2,3]

Received: 7 April 2020 / Accepted: 15 May 2020

Abstract
Optically transparent, urea (5 wt%)-doped triglycine sulphate (Ur-TGS) single crystals were grown along polar axis [010] by Sankaranarayanan–Ramasamy unidirectional solution growth method, below and above its Curie temperature $T_c = 49.3$ °C. Higher growth rate of 5 mm/day was obtained for Ur-TGS crystal grown above T_c. The phase of the grown crystals was confirmed by powder XRD. *P–E* hysteresis studies show well-saturated hysteresis loop for crystal grown below T_c, and the remnant polarization was 0.60 μC/cm^2 with a coercive field of 1.5 kV/cm. The piezoelectric d_{33} coefficient for Ur-TGS crystal grown below and above T_c was 25 pC/N and 35 pC/N, indicating improved piezoelectric properties of the latter. Dielectric permittivity for Ur-TGS crystal grown above T_c was approximately 10 times higher as compared to the crystal grown below T_c. Improved Vickers microhardness and lower Meyer's index (n) were observed for Ur-TGS crystal grown above T_c. The etch pit density (EPD) of Ur-TGS crystal grown below and above T_c was 1.8 and 1.1×10^2 dislocations/cm^2, respectively, indicating that the quality of the crystals grown above T_c was better than the crystal grown below T_c. The optical transmittance of Ur-TGS crystal grown above T_c was slightly (~5%) more than that of crystal grown below T_c. Overall, it is concluded that the higher growth rate and improved physical properties of Ur-TGS crystal grown above its Curie temperature show its suitability for the ferroelectric device applications.

Keywords Crystal growth · Triglycine sulphate (TGS) · Unidirectional solution growth · Sankaranarayanan–Ramasamy method · Curie temperature · Ferroelectric · Hysteresis

1 Introduction

Triglycine sulphate (TGS) is one of the most well-studied ferroelectric materials, especially because of its excellent ferroelectric, piezoelectric, pyroelectric and dielectric properties. It undergoes a second-order (order–disorder type) continuous phase transition at 49.3 °C. Below this temperature, the crystal exhibits ferroelectric phase, whereas above it the crystal gets transformed to the paraelectric phase. It belongs to monoclinic crystal system in both the phases but has a non-centrosymmetric space group $P2_1$ in the ferroelectric phase and centrosymmetric space group $P2_1/m$ in the paraelectric phase [1]. Due to its self-poling nature, it does not require any specific poling when it is cooled from the high-temperature phase to the low-temperature phase. Several different dopants have been tried in the past to improve the growth rate [2–4]. The effect of doping urea into TGS crystal has been studied by slow evaporation solution growth technique [5]. It was found that doping with urea increases the normalized growth yield significantly compared to pure TGS crystals, and an improvement in the ferroelectric, piezoelectric and dielectric values was also observed after doping. An important device made using TGS crystals is a pyroelectric sensor-based laser energy meter for detecting infrared (IR) radiations. However, a serious limitation of conventionally grown natural

✉ Muthu Senthil Pandian
senthilpandianm@ssn.edu.in

Sunil Verma
sverma1118@gmail.com

[1] SSN Research Centre, SSN College of Engineering, Kalavakkam, Chennai 603110, Tamil Nadu, India

[2] Laser and Functional Materials Division, Raja Ramanna Centre for Advanced Technology, Indore 452013, India

[3] Homi Bhabha National Institute, BARC Training School Complex, Anushakti Nagar, Mumbai 400094, India

Published online: 05 June 2020

morphology urea-doped TGS crystal and those grown preferentially along specific crystallographic directions is that the crystal has very small (010) face making it difficult to obtain large size device element. This results in very small percentage of the crystal usable for actual device applications. Very few reports in the literature have addressed this problem of increasing the (010) face area relative to other faces appearing in the TGS crystal morphology [6, 7]. In order to get TGS device element of desired size, length and orientation, we report in this paper unidirectional growth of [010]-oriented urea-doped TGS crystals below and above its Curie temperature. A comparative analysis of various physical properties such as ferroelectric *P–E* hysteresis loop, piezoelectric d_{33} coefficient, dielectric permittivity, mechanical stability and optical quality of [010]-oriented crystal elements obtained from these two crystals has also been performed.

2 Synthesis and conventional growth of pure and urea-doped TGS

TGS was synthesized using GR-grade (Merck, India) chemicals of glycine (NH_2CH_2COOH) and sulphuric acid (H_2SO_4) in the molar ratio 3:1 as follows:

$$3\underbrace{\left(NH_2CH_2COOH\right)}_{\text{Glycine}} + \underbrace{H_2SO_4}_{\text{Sulfuric acid}} \rightarrow \underbrace{2\left(NH_3^+CH_2COOH\right)\cdot\left(NH_3^+CH_2COO^-\right)\cdot SO_4^{2-}}_{\text{Triglycine Sulphate}}$$

The amount of dopant was 5 wt% urea, which was added to the mixture of glycine and sulphuric acid. After the reaction was complete, the TGS chemical was recrystallized twice before preparing the saturated solution. The solution was filtered using 0.2 µm membrane filter to eliminate the extraneous solid colloidal particles that can act as the source of spontaneous nucleation. The solubility of pure TGS is 36 g/100 ml at the temperature of 30 °C. But in the case of urea-doped TGS, the solubility in the below and above T_c region is 45 g/100 ml at 30 °C and 85 g/100 ml at 54 °C, respectively. The prepared solution was kept in a crystallizer covered with a perforated thick polyethylene sheet. The evaporation of the solvent at room temperature yielded TGS crystal in the time span of 15 days. A transparent and good optical quality crystal was obtained in this conventional growth method. The top- and side-view morphology of the grown TGS crystal is shown in Fig. 1. The morphologically important habit faces of pure TGS crystals are (001), (100), (010), (110), (-111) and (-1-11) [1]. Thermodynamic growth habit as shown in Fig. 1 is a reflection of crystallographic origin related to anisotropic chemical bonding along various planes, as clarified by the chemical bonding theory of single

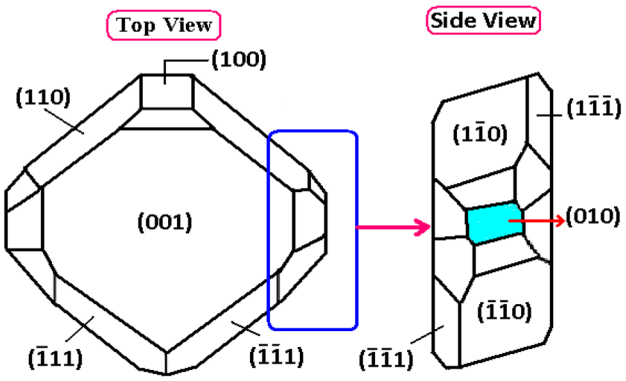

Fig. 1 Top and side view of the TGS morphology

crystal growth [8–10]. For this series of crystals, hydrogen bonds play a key role during nucleation and growth stages; urea thus can influence both morphologies and growth rates through multi-scale variations of the chemical bonding at individual faces [11, 12]. The morphology of urea-doped TGS crystals is different from pure TGS because the (010) face has minimum area as compared to other habit faces. The chemical bonding theory of single crystal growth [8–10] indicates that the fast growth along [010] is key to control crystal quality compared to other orientations.

3 [010] oriented urea-doped TGS crystal growth below and above T_c

A special growth apparatus was designed and fabricated for unidirectional growth of urea-doped TGS crystals. It consisted of helical shaped glass heaters filled with silicone oil and nichrome coil, which were placed inside beaker to function as water bath. A crystallizer in the shape of a conical glass ampoule of diameter 25 mm and length 150 mm was placed in the middle of helical heaters in the water bath. Using this design, two separate thermal zones were created vertically, one at top and another at bottom. The temperature of the two zones was controlled independently using two sets of PID temperature controller (Eurotherm 902P) and thyristor. The unidirectional growth apparatus for growth below and above T_c is shown in Fig. 2. A 3 mm long TGS seed crystal shaped as a cone along [010] axis was fixed using silicone sealant at the conical bottom of the glass ampoule.

The Curie temperature of TGS crystal is 49.3 °C. Since the growth was to be performed below the Curie point, the temperature at the top portion was maintained at 36 °C with an accuracy of ± 0.01 °C for the evaporation of the urea-doped TGS solution. A constant temperature of 28 °C was maintained at the bottom of the ampoule near the seed crystal for initiating the growth. Under these conditions, a highly transparent urea-doped TGS crystal of length 35 mm and

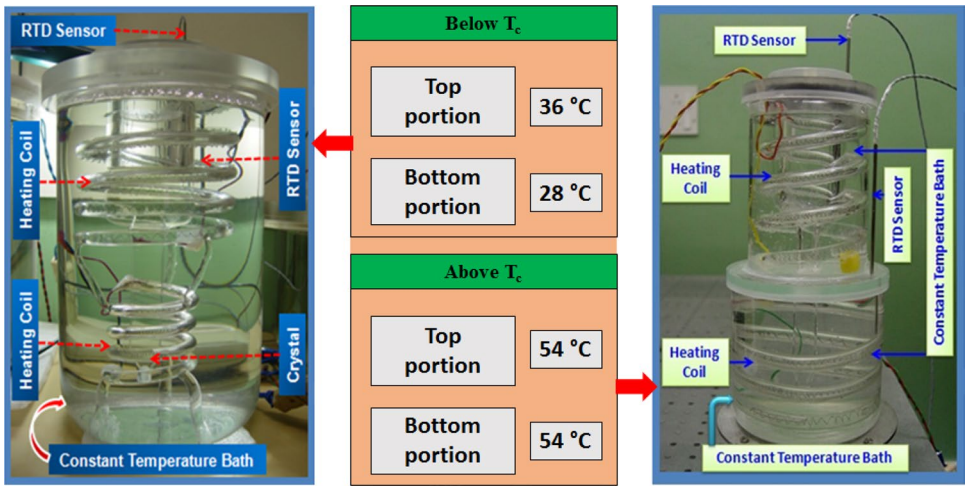

Fig. 2 SR crystal growth apparatus and temperature control instrumentation for below and above T_c

diameter 25 mm was grown within a period of 12 days. After completion of the growth run below T_c, the solution was removed from the growth ampoule and crystal was cooled to room temperature at a rate of 1 °C/hour to avoid any thermal shock. The grown TGS crystal was taken out from the glass ampoule using a diamond cutter. The [010]-oriented urea-doped TGS crystal inside and outside the ampoule is shown in Fig. 3a, b, and the wafer obtained from the crystal after cutting and polishing is shown in Fig. 3c, respectively. The growth rate of the below T_c grown Ur-TGS crystal was found to be 3 mm/day.

In order to perform growth above Curie temperature, a 5 mm long TGS seed crystal oriented along [010] direction was prepared from TGS crystal grown by conventional slow evaporation method. A cone-shaped TGS crystal was mounted at the bottom of the growth ampoule such that the (010) face was horizontal and facing upwards. The 250 ml of Ur-TGS saturated solution was prepared at 54 °C (above T_c) and poured in the glass ampoule. In order to achieve fast growth rate, which was possible due to higher solubility of the TGS above 50 °C, the solution was provided slow cooling from 54 to 50 °C in a programmed manner.

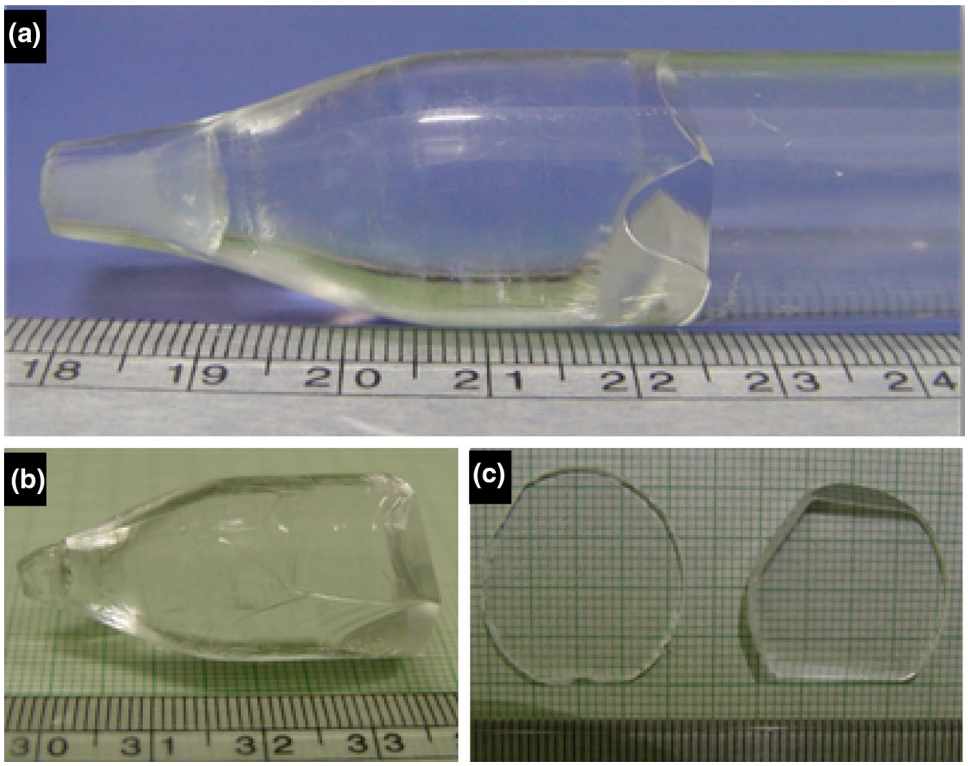

Fig. 3 Photograph of the Ur-TGS crystal grown below T_c oriented along [010] polar axis: **a** inside and **b** outside the glass ampoule and **c** (010) plates cut and polished from the grown Ur-TGS crystal

A cooling rate of 0.01 °C/h was used in the beginning, which was increased as the crystal grew in size. A highly transparent Ur-TGS crystal of 70 mm length along [010] direction and 15 mm diameter was grown in 14 days. After completion of the growth runs above T_c, the solution was removed from the ampoule and crystal was cooled to room temperature at a rate of 1 °C/h to avoid any thermal shock. The grown TGS crystal was taken out from the glass ampoule, and several samples were cut using diamond cutter. The grown crystal inside and outside the ampoule is shown in Fig. 4a, b, and several cut and polished ingots of Ur-TGS crystal grown above T_c are shown in Fig. 4c. The average growth rate achieved was 5 mm/day.

The average growth rate reported in the literature for a pure TGS crystal grown below T_c is 1 mm/day [7]. Comparing the growth rate data of Ur-TGS with that of pure TGS, it is found that the normalized growth rate along [010] direction of urea-doped TGS crystal grown below T_c is three times higher than pure TGS crystals and that grown above T_c is five times higher. This has implications for growing larger TGS crystals in the same amount of time keeping the other growth parameters same. The results show that the specific nature of growth in unidirectional growth method yields high percentage of material available for device application.

4 Sample preparations for characterizations

In order to perform comparative investigations of the various properties of the Ur-TGS crystals grown below and above T_c, samples in the form of thin plates were cleaved perpendicular to the *b*-axis [i.e. (010) slices] of the two crystals. The samples were lapped and polished using alumina powder and ethylene glycol. It was ensured that the thickness of the sample plates cleaved from the two crystals was identical. The reproducibility of the characterization results was confirmed by measuring the properties multiple times and ensuring that identical results were obtained.

4.1 Powder x-ray diffraction

To investigate the phase of the grown crystals, X-ray diffraction (XRD) was performed on powdered samples obtained from small crystalline samples of pure and Ur-TGS crystals grown below T_c. The diffracted beam was recorded by scanning the detector on a circular path from 20° to 70° with a scan speed of 2°/min. The diffraction patterns of Ur-TGS and pure TGS are shown in Fig. 5a, b, respectively. The number of peaks observed in urea-doped TGS crystal is higher than those in pure TGS, which are attributed to incorporation of urea dopant into the TGS crystal lattice. The prominent peaks of pure and Ur-TGS crystal are corresponding to (101), (220), (121), (040), (231) and (072) diffraction planes. The sharpness of peaks and small full-width at half maximum (FWHM) shows that the grown crystal has good phase purity.

4.2 Ferroelectric *P–E* hysteresis loop analysis

To investigate the ferroelectric properties, Ur-TGS sample plates oriented normal to the polar axis [010] were used to measure polarization as a function of the applied electric field, i.e. *P–E* hysteresis loop. The cut and polished Ur-TGS wafers of 1 mm thickness were coated with gold electrodes

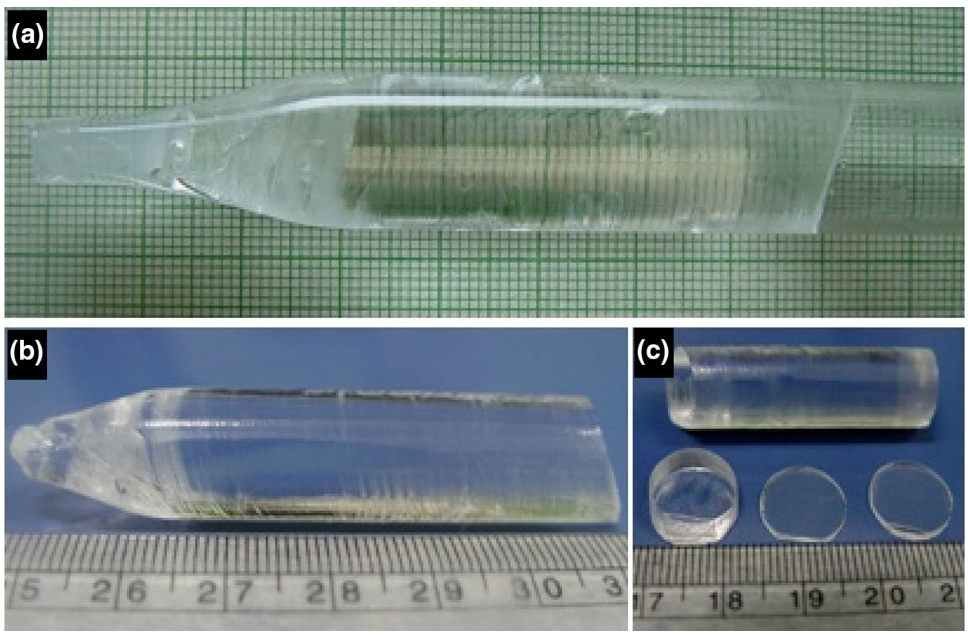

Fig. 4 Photograph of the Ur-TGS crystal grown above T_c oriented along [010] polar axis: **a** inside, **b** outside the glass ampoule and **c** (010)-oriented ingot and plates cut and polished from the grown Ur-TGS crystal

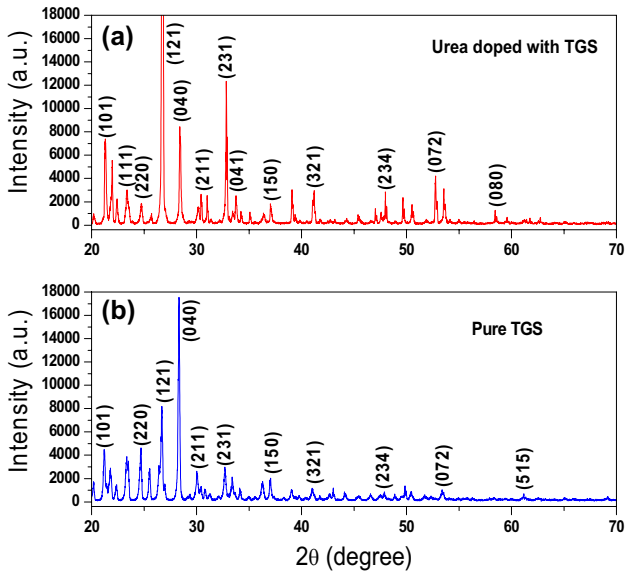

Fig. 5 Powder X-ray diffraction pattern of **a** Ur-TGS and **b** pure TGS and grown above T_c

for the purpose of electric field application. Hysteresis loops were measured with the help of Sawyer–Tower circuit [13] up to a maximum of 2.5 kV voltage using the Precision Work Station of the Radiant Technology Inc. The relationship between the remnant polarization (P_r), saturation polarization (P_s) and polarization at fields above coercive field is given by [14]

$$R_{sq} = \frac{P_r}{P_s} + \frac{P_{1.1E_c}}{P_r}$$

where R_{sq} and $P_{1.1E_c}$ are the squareness of hysteresis loop and polarization at an electric field equal to 1.1 times the coercive field, respectively. Using the above relationship, the *P–E* hysteresis behaviour of the Ur-TGS crystal grown in temperature regimes below and above the TGS Curie temperature (T_c = 49.3 °C) was investigated. The recorded ferroelectric hysteresis loops for Ur-TGS crystals grown below and above T_c are shown in Fig. 6a, b, respectively. The room temperature (30 °C) values of remnant polarization (P_r), saturation polarization (P_s) and coercive field (E_c) of the two type of Ur-TGS crystal grown by unidirectional growth method are presented in Table 1. The crystal grown below T_c was able to sustain a field up to 2.5 kV/cm, and the value of remnant polarization is 0.60 μC/cm^2. In addition, a well-saturated hysteresis loop was obtained. In the case of Ur-TGS crystal grown above T_c, the values of P_r decrease and E_c increase. The remnant polarization (P_r) was 0.0036 μC/cm^2, and coercive field (E_c) was 4.07 kV/cm for this crystal. It was observed that above T_c grown Ur-TGS crystal does not show saturation in polarization, which suggests that when the crystal is cooled from the paraelectric phase

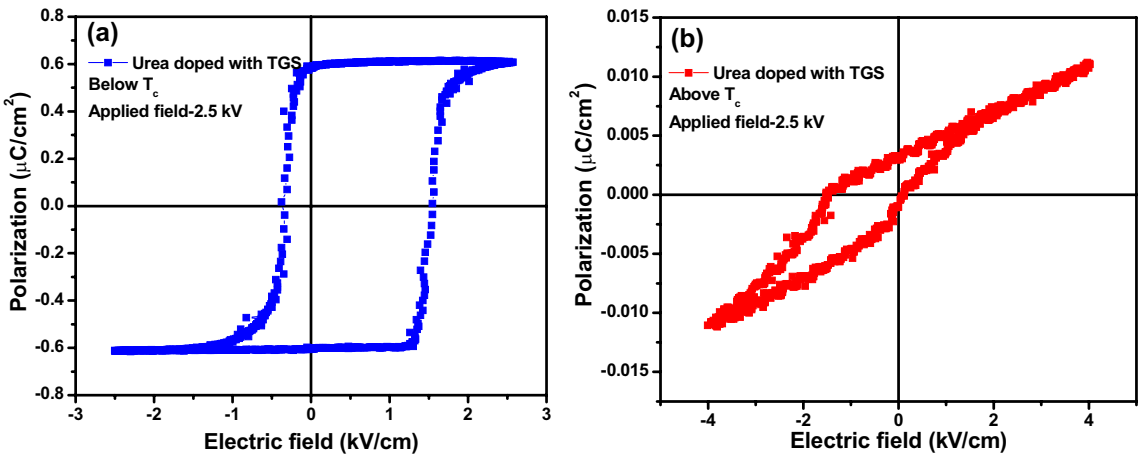

Fig. 6 *P–E* hysteresis loop of Ur-TGS crystal grown **a** below and **b** above T_c

Table 1 P–E hysteresis values of [010]-oriented Ur-TGS crystals grown below and above T_c

Name of the crystal	P_r (μC/cm^2)	P_s (μC/cm^2)	E_c (kV/cm)	$-E_c$ (kV/cm)
Ur-TGS below T_c	0.60	0.62	+1.5	−0.5
Ur-TGS above T_c	0.0036	–	4.07 (unsaturated value)	−4.01 (unsaturated value)

(54 °C) to ferroelectric phase (30 °C), the dipole moments of the domains behave differently which influence the ferroelectric hysteresis property.

4.3 Piezoelectric d_{33} coefficient

Piezoelectric coefficient (d_{33}) is an important parameter for sensor and transducer device applications. The d_{33} coefficient was measured using a piezometer for (010) habit face of the Ur-TGS crystals grown below and above T_c. A precision force generator was used to apply a calibrated force of 0.25 N at a frequency of 110 Hz that generated a charge on the crystal sample under test. The measured piezoelectric charge coefficients for Ur-TGS crystal grown below and above T_c were 25 pC/N and 35 pC/N, respectively, which are higher than the reported value of 18 pC/N for d_{33} coefficient of pure TGS crystal [7]. The higher d_{33} value of Ur-TGS crystals offers a good potential for applications in piezoelectric sensor and actuator devices. Further, since the piezoelectric properties are affected by defects such as dislocations [15], which cause slowing down of the domain wall mobility and tends to reduce the piezoelectric charge coefficient [16], higher values obtained for the grown Ur-TGS crystals suggest that the defects density was lower, and hence, the crystal quality was better.

4.4 Dielectric permittivity measurement

The Ur-TGS crystal plate was coated with gold on both side to form electrodes. The coating was done in argon atmosphere by using a sputtering unit (Emitech K 550X model, UK). The dielectric permittivity (ε_r) was determined at different temperatures in the frequency range of 100 Hz to 1 MHz using Hewlett Packard 4194A Impedance/Gain phase analyser. The variation of dielectric permittivity of Ur-TGS crystal grown below and above T_c in the above frequency range at different temperatures is shown in Fig. 7a, b, respectively. No distinct change in the ferroelectric phase transition temperature could be observed in the two types of samples. The Curie point was observed at ~ 49.3 °C in both the cases. Behaviour of ε_r as a function of temperature shows that ε_r of both the Ur-TGS crystals increases with increase in temperature up to ~ 49.3 °C and has maximum value at the Curie temperature. The dielectric permittivity of Ur-TGS crystal grown below T_c was found to be 205 at 49.3 °C and 100 Hz, whereas the value for the crystal grown above T_c was 1945, approximately 10 times more. For both the crystal samples, a sharp peak was observed in the temperature versus dielectric permittivity curve. The sharp peak is a signature of homogeneous and strain-free crystals. It is reported in the literature that ε_r of pure TGS crystal grown along (010) face is 64.2 [7]. Therefore, ε_r value of Ur-TGS crystals grown below and above T_c is much higher than that of pure TGS due to the doping of urea into TGS. Similar effects of doping were reported by Batra et al. in TGS crystals doped with samarium (Sm), although the change in the dielectric values in the present study is much larger [17]. The higher values of dielectric permittivity at lower frequencies may be attributed to the composition-related space charge polarization which depends on the purity and lattice defects of the crystal sample [18, 19].

4.5 Vickers microhardness

In general, infrared detector devices require TGS crystal in the form of plates of thickness ~ 10 µm. Therefore, in determining the fabrication and possible device applications, the mechanical properties of the grown Ur-TGS crystals

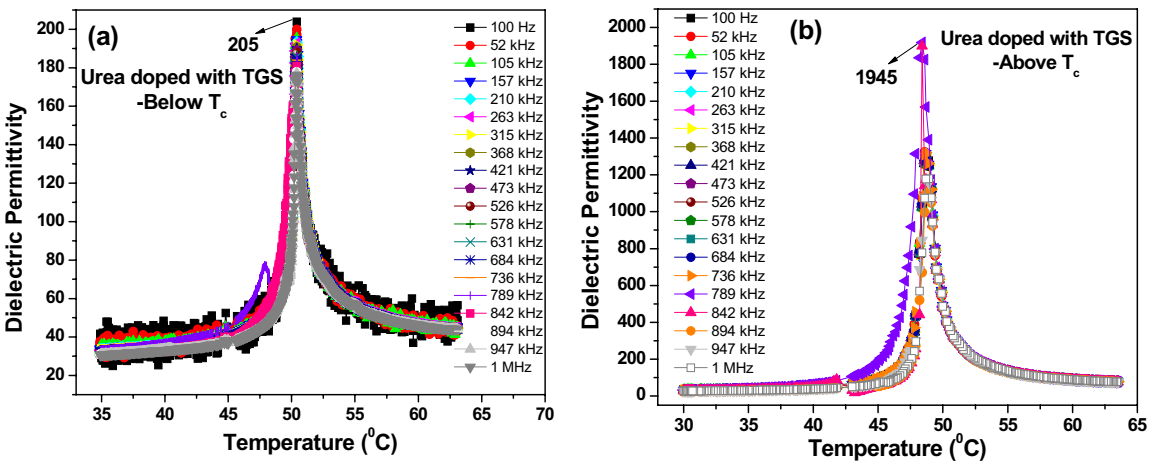

Fig. 7 Temperature-dependent dielectric permittivity of Ur-TGS crystal grown **a** below and **b** above T_c

and their strength are of vital importance. Microhardness measurements were taken on the (010) face using hardness tester (Matsuzawa MMTX-7, Japan) fitted with a diamond pyramidal indenter with a constant indentation time of 5 s. Two-millimetre-thick (010) plate from Ur-TGS crystal and the load ranging from 10 to 200 g was used. The hardness number (H_v) was calculated using the formula:

$$H_v = (1.854\ P)/d^2 \quad \left(\mathrm{kg/mm^2}\right)$$

where H_v is the Vickers hardness number (kg/mm^2), P is the applied load (g), and d is the average diagonal length (mm) of the indentation mark. A plot of the microhardness as a function of the applied load clearly indicates that hardness of the below and above T_c grown crystal increases with increase in load up to 100 g and above that H_v decreases suddenly. When indenter just touches the surface of the Ur-TGS crystal, dislocations are generated in the indented region, so H_v increases initially. Above 100 g of load, the H_v decreases due to the increase in diagonal length of the indentation (d) and mutual interactions of dislocations [20]. The microhardness values of below and above T_c grown Ur-TGS crystals are 63.9 kg/mm^2 and 129.5 kg/mm^2, respectively, at 100 g of load (Fig. 8a). Intrinsically, the mechanical hardness of crystals is anisotropically related to their various microscopic structures such as bond strength [21–23]. This large increase in the microhardness in above T_c grown Ur-TGS crystal may be attributed to the fact that urea could intercalate with the formation of new H-bonds into the crystalline lattice and enhance the mechanical stability.

Cracks were formed near indentation point when load exceeded 100 g, which tend to propagate when the load increased to 200 g, as evident from Fig. 9. At lower loads, such impression appears to be free of cracks, but for loads greater than 100 g microcracks were well defined. Analysis of the hardness measurement results reveals that decrease in hardness was more for Ur-TGS crystal grown above T_c as compared to that grown below T_c. It is reported in the literature that crystals with higher hardness develop more cracks around the indentation mark [24, 25]. This is the main reason for higher reduction of hardness above 100 g of load in above T_c grown crystal. The prominent microcracks around the indentation are higher in crystal grown above T_c as compared to that grown below T_c. A close observation of the indentation marks reveals that crack length is longer in above T_c grown crystal, which is due to the force of the diamond indenter causing more number of cracks in crystal grown above T_c.

The relationship between the applied load and the diagonal length 'd' of the indentation mark is given by Meyer's law $P = a \times d^{\,n}$, where 'n' is the Meyer's index or work

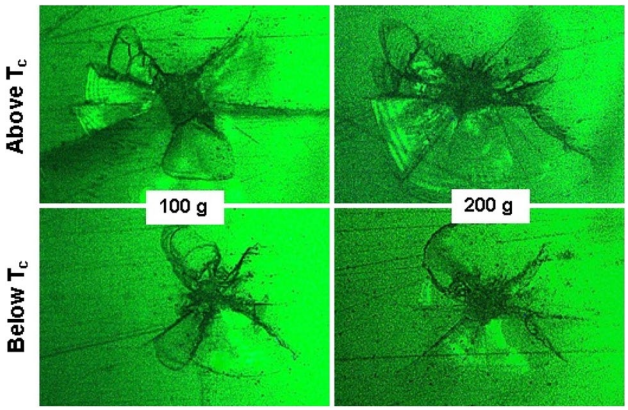

Fig. 9 Indentation patterns obtained in above and below T_c grown Ur-TGS crystal

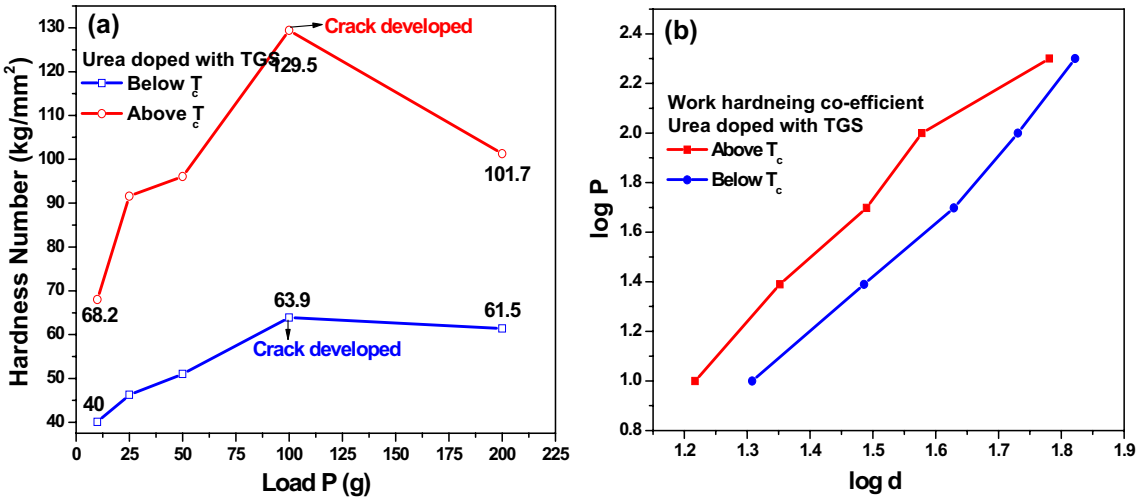

Fig. 8 **a** Load-dependent microhardness values and **b** work hardening coefficient values

hardening coefficient. This is calculated from the slope of straight line between log P and log d. Onitsch [26] and Hanneman [27] have reported that 'n' lies between 1 and 1.6 for moderately hard materials and it is more than 1.6 for soft materials. The value of work hardening coefficient obtained for Ur-TGS crystal grown below and above T_c is 1.5 and 1.3, respectively (Fig. 8b). Thus, both the Ur-TGS crystals belong to the category of hard materials. The increase in microhardness of Ur-TGS crystal grown above T_c is useful in mechanical processing of these crystals for obtaining (010)-oriented device elements for infrared detector fabrication.

4.6 Chemical etching

Chemical etching studies were carried out on the Ur-TGS crystals grown below and above T_c by unidirectional solution growth technique to study dislocation density. (010) plates from Ur-TGS crystals were etched for different durations, ranging from 4 to 15 s, using water as etchant. The etched surfaces were examined under an optical microscope (OLYMPUS U-TV0.5XC-3, Japan). The gradual dissolution of the Ur-TGS surface layers helped to distinguish between the pits corresponding to dislocations and those of from other structural defects. Figure 10a shows elongated oval-shaped etch pits developed on the surface after etching for 4 s. Randomly distributed but strictly oriented pits were observed. Figure 10b illustrates the etch pit pattern produced on the same surface after successive etching for 8 s. Increase in etching time does not change the morphology of the etch pit. On successive etching from 4 to 15 s, the elongated oval-shaped etch pits do not disappear suggesting that the etch pits are due to dislocations. In utilizing ferroelectric single crystals for IR applications, it is essential to grow single crystals containing a low dislocation density [28]. The estimated etch pit density (EPD) of below T_c grown Ur-TGS crystal was 1.8×10^2 cm^{-2}.

Compared to the crystal grown below T_c, the size of etch pits is slightly larger and the number of pits is lesser in Ur-TGS crystal grown above T_c. Figure 10c, d represents the identical elongated oval shaped etch pits observed on above T_c grown crystal after etching with water for 4 s and 8 s, respectively. The calculated EPD is 1.1×10^2 cm^{-2}. The difference between the EPD can be attributed to difference in growth condition such as below (36 °C) and above T_c (54 °C) which influences the crystalline perfection. The probable reason for lower EPD in the case of above T_c grown crystal is due to the good crystalline perfection which is in tune with higher piezoelectric (d_{33}), dielectric (ε_r) and mechanical (H_v) properties.

4.7 UV–Vis NIR analysis

The optical transmission of Ur-TGS crystal grown below and above T_c was measured using spectrophotometer (JASCO V-670) in the wavelength range 190 nm to 2200 nm. The scan parameters were: slit width 2 nm and scan speed 200 nm/min. Figure 11 shows that the transmission is nearly 86% for the 1 mm thick (010) plate of Ur-TGS crystal grown below T_c and the transmission of 91% for above T_c grown crystal of the same orientation and thickness. The UV transmittance of crystal grown above T_c is 5% higher than that of below T_c grown crystal, which can be attributed to absorption of UV radiation by impurities which get trapped in crystal growing at relatively lower temperatures [29, 30]. Dislocation in crystals affects the optical properties such as

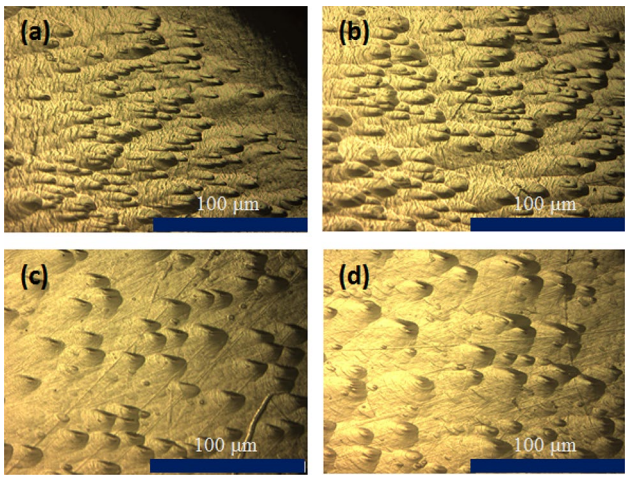

Fig. 10 Etch pit patterns of Ur-TGS crystal grown for below T_c (**a**, **b**) and above T_c (**b**, **d**) for 4 s and 8 s, respectively

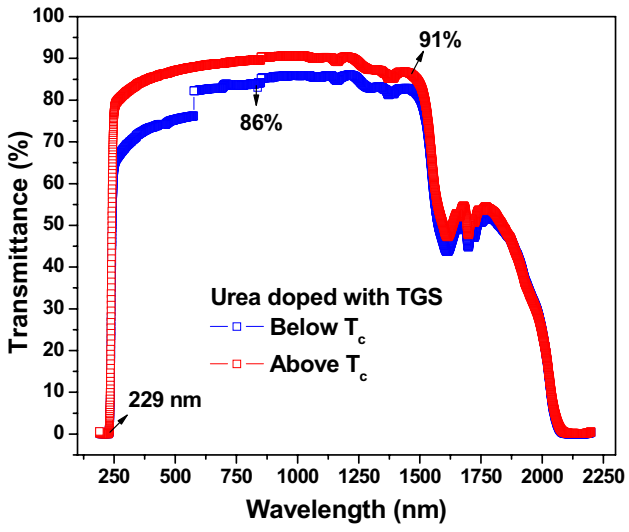

Fig. 11 UV–Vis–NIR optical transmittance measurements of (010)-oriented Ur-TGS crystals grown below and above TGS crystals

Table 2 Comparison of physical properties of [010]-oriented Ur-TGS crystal grown below and above T_c

Name of the measurements	Urea-doped TGS	
	Below T_c	Above T_c
Growth rate	3 mm/day	5 mm/day
Piezoelectric d_{33} coefficient	25 pC/N	35 pC/N
Dielectric permittivity at 49 °C	205	1945
Vickers microhardness at 10 g	40 kg/mm^2	68.2 kg/mm^2
Vickers microhardness at 100 g	63.9 kg/mm^2	129.5 kg/mm^2
Crack length at 100 g	32.36 µm	86.62 µm
Work hardening coefficient	1.5	1.3
Etch pit density (EPD)	1.8×10^2 cm^{-2}	1.1×10^2 cm^{-2}
Optical transmittance	86%	91%

light absorption, scattering, refractive index [31], and for device applications crystals free from scattering and absorption are required. It can be inferred that higher dislocation density leads to generation of scattering centres in the Ur-TGS crystal grown below T_c, which consequently decreases the optical transparency. This is in agreement with the etching studies.

By selecting dipolar impurity like urea, the figures of merit of TGS crystals for device applications have increased significantly. Urea-doped crystals have three times (below T_c) and five times (above T_c) higher normalized growth yield as compared to pure TGS reported elsewhere [7]. The comparative studies of ferroelectric, piezoelectric, dielectric, mechanical stability, optical quality and crystalline perfection of below and above T_c grown Ur-TGS crystals reveal that above T_c grown Ur-TGS crystals have better physical properties, better crystal quality and most importantly higher growth rate. The comparison of physical properties of [010]-oriented Ur-TGS crystal grown below and above T_c is given in Table 2.

5 Conclusions

The salient conclusions of the present study are summarized below:

(i) *Crystal growth*: 5 wt% urea-doped triglycine sulphate (Ur-TGS) single crystals were successfully grown along polar axis [010] by unidirectional solution growth method (Sankaranarayanan–Ramasamy method) in two temperature ranges: one below its Curie temperature T_c (49.3 °C) and another above it. Specialized apparatus was fabricated for the growth experiments. Growth rate of Ur-TGS crystal grown below T_c was 3 mm/day, whereas that grown above T_c was 5 mm/day. The phase of the grown crystals was confirmed by powder XRD.

(ii) *P–E hysteresis measurements*: *P–E* hysteresis studies of Ur-TGS crystal grown below T_c show well-saturated hysteresis loop and the remnant polarization was 0.60 µC/cm2 with a coercive field of 1.5 kV/cm. Unsaturated hysteresis behaviour was observed for crystal grown above T_c, up to the maximum applied electric field of 2.5 kV/cm.

(iii) *Piezoelectric studies*: The d_{33} values of Ur-TGS crystal grown below and above T_c were 25 pC/N and 35 pC/N. The d_{33} coefficient indicates that the piezoelectric property of the above T_c grown crystal was better.

(iv) *Dielectric permittivity*: Nearly 10 times higher dielectric permittivity was observed for Ur-TGS crystal grown above T_c as compared to the crystal grown below T_c.

(v) *Microhardness studies*: Higher value of microhardness (H_v) and lower value of Meyer's index (n) were observed for Ur-TGS crystal grown above T_c.

(vi) *Defects density:* The etch pit density (EPD) of Ur-TGS crystal grown below and above T_c was 1.8 and 1.1×10^2 dislocations/cm^2, respectively. Less number of etch pits in crystal grown above T_c shows that the quality of the crystals grown above T_c is better than the crystal grown below T_c.

(vii) *Optical transmittance*: The optical transmittance Ur-TGS crystal grown above T_c is slightly (~5%) more than that of crystal grown below.

Therefore, higher growth rate and improved physical properties of Ur-TGS crystal grown above its Curie temperature show its higher potential for device applications.

Acknowledgements M. Senthil Pandian is grateful to RRCAT authorities for granting six months project. Authors gratefully acknowledge Late Dr. R. Gopalakrishnan for Vickers microhardness measurements. P. Karuppasamy is thanked for his help in redrawing a few figures.

References

1. A. Saxena, V. Gupta, K. Sreenivas, Dielectric and ferroelectric properties of phosphoric acid doped triglycine sulfate single crystals. Mater. Sci. Eng., B **79**, 91 (2001)
2. S.C. Mathur, A.K. Batra, A. Mansingh, Studies on triglycine sulphate crystals doped with nitroanilines. J. Phys. D Appl. Phys. **13**, 79 (1980)
3. T. Kikuta, A. Takagi, T. Yamazaki, N. Nakatani, Growth and internal bias field of L-lysine-doped triglycine sulfate (LLysTGS). J. Cryst. Growth **307**, 372 (2007)
4. N. Nakatani, T. Kikuta, T. Yamazaki, Growth and domain structure of TGS crystals doped with various amino acids. Ferroelectrics **368**, 12 (2008)

5. J.M. Chang, A.K. Batra, R.B. Lal, Growth and properties of urea-doped triglycine sulfate (UrTGS) crytals. J. Cryst. Growth **158**, 284 (1996)
6. M. Senthil Pandian, N. Balamurugan, V. Ganesh, P.V. Raja Shekar, K. Kishan Rao, P. Ramasamy, Growth of TGS single crystal by conventional and SR method and its analysis on the basis of mechanical, thermal, optical and etching studies. Mater. Lett. **62**, 3830 (2008)
7. M. Senthil Pandian, P. Ramasamy, B. Kumar, A comparative study of ferroelectric triglycine sulfate (TGS) crystals grown by conventional slow evaporation and unidirectional method. Mater. Res. Bull. **47**, 1587 (2012)
8. C. Sun, D. Xue, Chemical bonding theory of single crystal growth and its application to crystal growth and design. CrystEngComm **18**, 1262 (2016)
9. C. Sun, D. Xue, Chemical bonding theory of single crystal growth and its application to ϕ 3″ YAG bulk crystal. CrystEngComm **16**, 2129 (2014)
10. C. Sun, D. Xue, Pulling growth technique towards rare earth single crystals. Sci. China Technol. Sci. **61**, 1295 (2018)
11. C. Sun, D. Xue, Perspectives of multiscale rare earth crystal materials. CrystEngComm **21**, 1838 (2019)
12. C. Sun, D. Xue, Chemical bonding in micro-pulling down process: high throughput single crystal growth. Sci. China Technol. Sci. **61**, 1776 (2018)
13. C.B. Sawyer, C.H. Tower, Rochelle salt as a dielectric. Phys. Rev. **35**, 269 (1930)
14. J. Novonty, J. Zelinka, Z. Podvalova, Growth and characterization of TGS single crystals doped with D-phenylalanine and Pt(IV) ions. Ferroelectrics **313**, 1 (2004)
15. A. Saxena, V. Gupta, K. Sreenivas, Characterization of phosphoric acid doped TGS single crystals. J. Cryst. Growth **263**, 192 (2004)
16. X. Guisheng, L. Haosu, W. Pingchu, X. Haiqing, Y. Zhiwen, Ferroelectric and piezoelectric properties of novel relaxor ferroelectric single crystals PMNT. Chin. Sci. Bull. **45**, 491 (2000)
17. A.K. Batra, P. Guggilla, D. Cunningham, M.D. Aggarwal, R.B. Lal, Growth and characterization of rare earths doped triglycine sulfate crystals. Phys. B **371**, 210 (2006)
18. I.G. Austin, N.F. Mott, Polarons in crystalline and non-crystalline materials. Adv. Phys. **18**, 41 (1969)
19. D. Xue, K. Kitamura, Dielectric characterization of the defect concentration in lithium niobate single crystals. Solid State Commun. **122**, 537 (2002)
20. M. Senthil Pandian, N. Balamurugan, G. Bhagavannarayana, P. Ramasamy, Characterization of < 0 1 0 > directed KAP single crystals grown by Sankaranarayanan–Ramasamy (SR) method. J. Cryst. Growth **310**, 4143 (2008)
21. M. Senthil Pandian, K. Boopathi, P. Ramasamy, G. Bhagavannarayana, The growth of benzophenone crystals by Sankaranarayanan–Ramasamy (SR) method and slow evaporation solution technique (SEST): a comparative investigation. Mater. Res. Bull. **47**, 826 (2012)
22. K. Li, X. Wang, F. Zhang, D. Xue, Electronegativity identification of novel superhard materials. Phys. Rev. Lett. **100**, 235504 (2008)
23. K. Li, P. Yang, D. Xue, Anisotropic hardness prediction of crystalline hard materials from the electronegativity. Acta Mater. **60**, 35 (2012)
24. S. Yu Boyarskaya, S.S. Shutova, R.P. Zhitaru, Inversion of dislocation rosettes in NaCl single crystals. Phys. Status Solidif. **30**, K7 (1975)
25. M. Senthil Pandian, N. Pattanaboonmee, P. Ramasamy, P. Manyum, Studies on conventional and Sankaranarayanan–Ramasamy (SR) method grown ferroelectric glycine phosphite (GPI) single crystals. J. Cryst. Growth **314**, 207 (2011)
26. E.M. Onitsch, Mikroscopia **2**, 131 (1947)
27. M. Hanneman, Metall. Manch. **23**, 135 (1941)
28. M. Senthil Pandian, P. Ramasamy, Sodium sulfanilate dihydrate (SSDH) single crystals grown by conventional slow evaporation and Sankaranarayanan–Ramasamy (SR) method and its comparative characterization analysis. Mater. Chem. Phys. **132**, 1019 (2012)
29. I.M. Pritula, Y.N. Velikhov, Some aspects of UV absorption of NLO KDP crystals. Proc. SPIE **202**, 3793 (1999)
30. M. Senthil Pandian, P. Ramasamy, Conventional slow evaporation and Sankaranarayanan–Ramasamy (SR) method grown diglycine zinc chloride (DGZC) single crystal and its comparative study. J. Cryst. Growth **312**, 413 (2010)
31. N.B. Singh, T.A. Gould, R.H. Hopkins, Etching studies on crystal of thallium arsenic selenide. J. Cryst. Growth **78**, 43 (1986)